Synthesis, Spectroscopy and Catalysis of [Cr(acac)$_3$] Complexes Grafted onto MCM-41 Materials: Formation of Polyethylene Nanofibres within Mesoporous Crystalline Aluminosilicates

Bert M. Weckhuysen,*[a] R. Ramachandra Rao,[a] Josephina Pelgrims,[a] Robert A. Schoonheydt,[a] Philippe Bodart,[b] Guy Debras,[b] Olivier Collart,[c] Pascal Van Der Voort,[c] and Etienne F. Vansant[c]

Abstract: Chromium acetyl acetonate [Cr(acac)$_3$] complexes have been grafted onto the surface of two mesoporous crystalline materials; pure silica MCM-41 (SiMCM-41) and Al-containing silica MCM-41 with an Si:Al ratio of 27 (AlMCM-41). The materials were characterized with X-ray diffraction, N_2 adsorption, thermogravimetrical analysis, diffuse reflectance spectroscopy in the UV-Vis-NIR region (DRS), electron spin resonance (ESR) and Fourier transform infrared spectroscopy. Hydrogen bonding between surface hydroxyls and the acetylacetonate (acac) ligands is the only type of interaction between [Cr(acac)$_3$] complexes and SiMCM-41, while the deposition of [Cr(acac)$_3$] onto the surface of AlMCM-41 takes place through either a ligand exchange reaction or a hydrogen-bonding mechanism. In the as-synthesized materials, Cr^{3+} is present as a surface species in pseudo-octahedral coordination. This species is characterized by high zero-field ESR parameters D and E, indicating a strong distortion from O_h symmetry. After calcination, Cr^{3+} is almost completely oxidized to Cr^{6+}, which is anchored onto the surface as dichromate, some chromate and traces of small amorphous Cr_2O_3 clusters and square pyramidal Cr^{5+} ions. These materials are active in the gas-phase and slurry-phase polymerization of ethylene at 100 °C. The polymerization activity is dependent on the Cr loading, precalcination temperature and the support characteristics; a 1 wt % [Cr(acac)$_3$]-AlMCM-41 catalyst pretreated at high temperatures was found to be the most active material with a polymerization rate of 14000 g polyethylene per gram of Cr per hour. Combined DRS-ESR spectroscopies were used to monitor the reduction process of $Cr^{6+/5+}$ and the oxidation and coordination environment of Cr^{n+} species during catalytic action. It will be shown that the polymer chains initially produced within the mesopores of the Cr-MCM-41 material form nanofibres of polyethylene with a length of several microns and a diameter of 50 to 100 nanometers. These nanofibres (partially) cover the outer surface of the MCM-41 material. The catalyst particles also gradually break up during ethylene polymerization resulting in the formation of crystalline and amorphous polyethylene with a low bulk density and a melt flow index between 0.56 and 1.38 g per 10 min; this indicates the very high molecular weight of the polymer.

Keywords: aluminosilicates · catalysis · chromium · mesoporosity · polyethylene

Introduction

In the early 1990s, Kresge and co-workers at Mobil reported the preparation of a new class of silica- and silica-alumina-based molecular sieves by using surfactant template molecules.[1, 2] The so-called M41S materials possess a periodic framework of regular mesopores, the size of which depends on the alkyl chain length of the template molecule. This discovery has greatly expanded the range of potential catalysts and catalyst supports.

MCM-41 is the most prominent example of this M41S family and can be envisaged as a hexagonal tubular material with a very high surface area and with sharply defined pore

[a] Dr. B. M. Weckhuysen, Dr. R. Ramachandra Rao, J. Pelgrims, Prof. Dr. R. A. Schoonheydt
Centrum voor Oppervlaktechemie en Katalyse
Departement Interfasechemie, K.U.Leuven
Kardinaal Mercierlaan 92, 3001 Leuven, Heverlee (Belgium)
Fax: (+32) 1632-1998
E-mail: bert.weckhuysen@agr.kuleuven.ac.be

[b] Dr. P. Bodart, Dr. G. Debras
Polyolefins Development Department, Fina Research
Zone Industrielle C, 7181 Seneffe, Feluy (Belgium)

[c] O. Collart, Dr. P. Van Der Voort, Prof. Dr. E. F. Vansant
Laboratorium voor Adsorptie en Katalyse
Departement Scheikunde, Universiteit Antwerpen (U.I.A.)
Universiteitsplein 1, 2610 Wilrijk (Belgium)

  0947-6539/00/0616-2960 $ 17.50+.50/0

diameters in the range of 2–10 nm. Pure silica MCM-41 possesses a neutral framework, which limits its application as a catalyst or as a support for preparing novel heterogeneous catalysts. When trivalent cations such as Al^{3+}, B^{3+} or Ga^{3+} are substituted for Si^{4+} in the walls of MCM-41, the framework possesses negative charges that can be compensated by protons; this results in materials useful for acid-catalyzed reactions.[3–7] Redox activity is obtained when a transition metal ion, such as Ti^{3+}, Mn^{2+} or Cr^{3+}, is introduced during synthesis in the MCM-41 material.[3–6, 9–13] Possible reactions include the oxidation of cyclohexene over Ti-MCM-41 in the presence of hydrogen peroxide[5] and the epoxidation of stilbene over Mn-MCM-41 in the presence of *tert*-butyl hydroperoxide.[12] A disadvantage of these materials prepared by direct synthesis is that not all the active sites are accessible for catalysis because the metal ions are partially located inside the walls of MCM-41.

Another preparation method is grafting the active species onto the inner surface of the mesopores of the MCM-41 material. In this case, all catalytically active sites are (in principle) accessible. Recently, we briefly reported on the polymerization of ethylene over well-defined chromium complexes grafted onto MCM-41.[14] It was shown that chromium acetylacetonate [$Cr(acac)_3$] complexes can be grafted onto the surface of Al-MCM-41 materials, giving rise to materials active in the polymerization of ethylene.

A detailed characterization study of these novel polymerization catalysts is presented here. The Cr-MCM-41 materials have been characterized with X-ray diffraction (XRD), N_2 adsorption, thermogravimetrical analysis (TGA), electron spin resonance (ESR), diffuse reflectance spectroscopy in the UV-Vis-NIR region (DRS) and Fourier transform infrared spectroscopy (FTIR), and tested regarding the polymerization of ethylene in both the gas and slurry phase. The polymers formed have been characterized with a melt flow indexer and by scanning electron microscopy (SEM), differential scanning calorimetry (DSC), XRD and FTIR. In addition, combined DRS/ESR spectroscopies have been used to monitor the Cr species during catalytic action.

Results and Discussion

Synthesis and physicochemical characterization of Cr-MCM-41 catalysts: An overview of the synthesized MCM-41 and Cr-MCM-41 materials, the sample notation and their physical properties is given in Table 1. The XRD patterns of the as-synthesized and calcined SiMCM-41 and AlMCM-41 were identical to those reported in the literature, confirming the hexagonal mesoporous structure.[1–5] The d-spacings (wall thickness + pore diameter) of calcined SiMCM-41 and AlMCM-41 were 39.2 and 37.1 Å, respectively. The pore size distribution of calcined SiMCM-41 and AlMCM-41 was very narrow with mean pore diameters of 25.0 and 29.5 Å, respectively, as determined by the BJH (Barrett, Joyner and Halenda) method.

No drastic changes in XRD peak positions and intensities and d-spacings were observed after grafting the MCM-41 materials with [$Cr(acac)_3$] complexes or after calcination of the [$Cr(acac)_3$]-MCM-41 materials in oxygen at either 550 or 720 °C. Table 1 indicates that: 1) the mean pore diameter and pore volume of the Cr-MCM-41 materials decrease slightly with increasing amounts of [$Cr(acac)_3$] complexes grafted onto the surface, 2) the initial pore sizes and pore volumes of the materials are almost completely restored after calcination at 550 °C and 3) calcination at 720 °C results in a reduction in the mean pore diameter and pore volume of the MCM-41 material.

The removal of the acetylacetonate (acac) ligands from the chromium complexes grafted onto the surface of MCM-41 has been studied by using TGA in oxygen. The TGA curves of 1.00-Si-A and 1.00-Al-A are compared in Figure 1. It is clear that the acac ligands are removed in two distinct stages. In the case of 1.00-Si-A, a first weight loss is observed in the temperature range between 190 and 270 °C, while the second weight loss takes place between 300 and 330 °C. The number of acac molecules per chromium atom was found to be 3.03, which indicates that there is only one type of Cr complex with three acac molecules on the surface (Figure 2). This complex most probably interacts with surface hydroxyl groups of the MCM-41 material through hydrogen bonding.

Sample 1.00-Al-A is characterized by a first weight loss between 210 and 280 °C, and a second one between 300 and 330 °C (Figure 1b). Here, the number of acac molecules per chromium atom was found to be 2.65. This number is indicative of the presence of two types of complexes on the MCM-41 surface. The first type of Cr complex has two acac ligands and, most probably, two additional oxygen ligands from the support. This complex is illustrated in Figure 3. It is the presence of Al in CrAlMCM-41 materials that results in

Table 1. Samples, sample notation and physicochemical properties.

Sample	Treatment[a]	Sample notation	d spacing [Å]	BET surface area [$m^2 g^{-1}$]	Mean pore diameter [Å]	Pore volume [$mL g^{-1}$]
SiMCM-41	C	0.00-Si-C	39.2	1360	25.0	1.03
AlMCM-41	C	0.00-Al-C	37.1	878	29.0	1.18
0.50 wt % Cr/AlMCM-41	A	0.50-Al-A	37.1	890	29.0	1.16
0.75 wt % Cr/AlMCM-41	A	0.75-Al-A	37.6	950	28.4	1.15
1.00 wt % Cr/AlMCM-41	A	1.00-Al-A	37.4	995	26.6	1.12
1.00 wt % Cr/AlMCM-41	C	1.00-Al-C	38.4	1070	28.0	1.42
1.00 wt % Cr/AlMCM-41	C720	1.00-Al-C720	37.8	987	24.7	1.05
1.50 wt % Cr/AlMCM-41	A	1.50-Al-A	37.4	965	25.4	1.09
2.00 wt % Cr/AlMCM-41	A	2.00-Al-A	37.7	1002	24.3	1.06
1.00 wt % Cr/SiMCM-41	A	1.00-Si-A	39.3	1260	23.7	0.93
1.00 wt % Cr/SiMCM-41	C	1.00-Al-C	40.3	1290	25.0	0.97

[a] C = calcined, A = as-synthesized.

  0947-6539/00/0616-2961 $ 17.50+.50/0

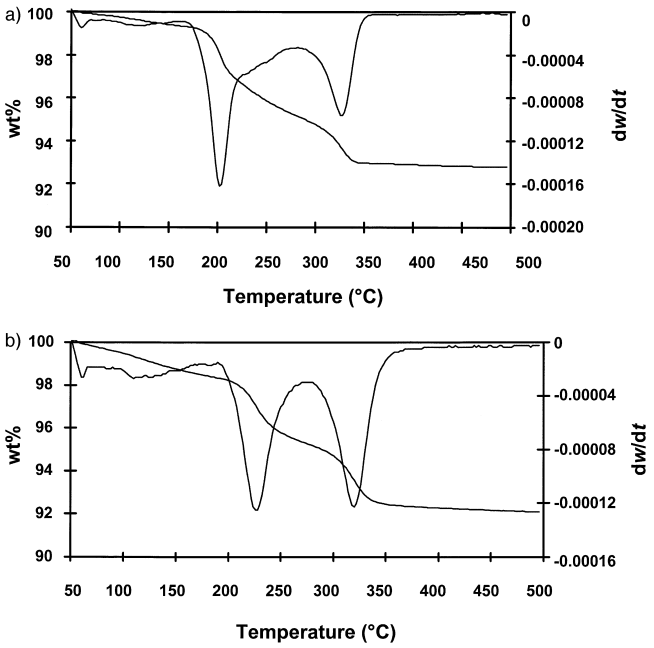

Figure 1. TGA analysis of a) sample 1.00-Si-A and b) sample 1.00-Al-A heated in O_2.

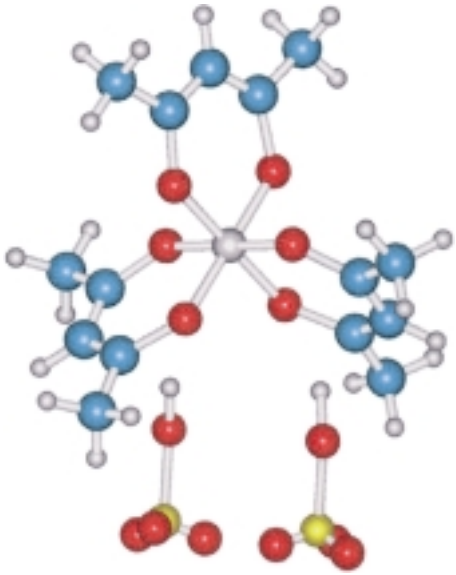

Figure 2. Cr complex with three acac ligands.

the ligand exchange reaction and, consequently, in the formation of covalent Cr–O–Al bonds. This can be explained by the acid character of the Al-OH groups present in this material. The second Cr complex contains three acac ligands, which have partial hydrogen bonding with framework hydroxyl groups (Figure 2). Thus, the deposition of $[Cr(acac)_3]$ complexes onto the surface of AlMCM-41 takes place through either hydrogen bonding between surface hydroxyls and the acac ligands of the complex, or a ligand exchange reaction with Al-OH groups.

These results are in close agreement with those reported by Haukka et al. and Babich et al. for $[Cr(acac)_3]$ complexes grafted on silica.[15, 16] According to Babich et al., two acac ligands are removed as acetylacetone in the first stage of the heat treatment, with the aid of the surface protons of the silica

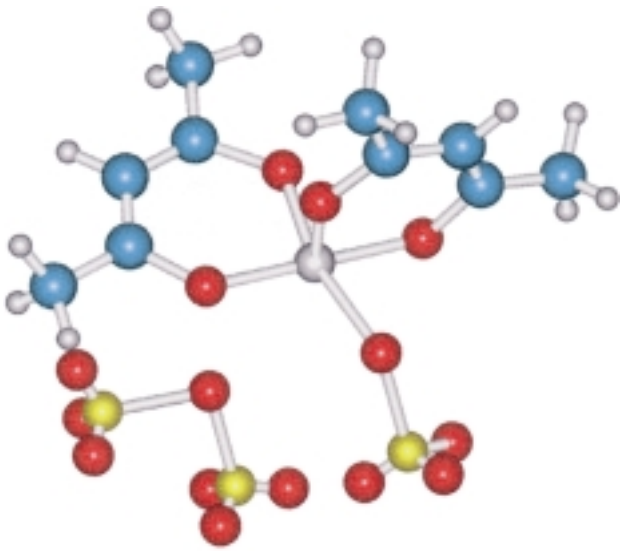

Figure 3. Cr complex with two acac ligands and two additional oxygen ligands from the support.

support. The second weight loss is due to the removal of the remaining acac ligands. Similarly, our data can be explained by assuming that in the first stage two acac ligands are removed as acetylacetone with the aid of surface hydroxyl groups of MCM-41. The remaining acac ligands are removed by an oxidation or pyrolysis process at 300–330 °C. However, hydrogen bonding between surface hydroxyls and acac ligands was considered to be the only type of interaction between $[Cr(acac)_3]$ complexes and silica. This is not the case for our Cr-AlMCM-41 samples (Figure 3).

Spectroscopy of Cr-MCM-41 catalysts: The as-synthesized $[Cr(acac)_3]$-MCM-41 catalysts of Table 1 were studied in detail with FTIR, DRS and ESR spectroscopies in order to study the decomposition mechanism of the deposited $[Cr(acac)_3]$ complexes on the MCM-41 surface and to elucidate the nature of the Cr species formed after calcination.

A series of FTIR spectra of the 1.00-Si-A sample obtained after different heat treatments in an in situ IR cell are given in Figure 4. The spectra were recorded at different temperatures in the presence of oxygen. The region between 1200 and 1900 cm^{-1}, which is characteristic for the vibrations of the acac ligands, is shown in Figure 4a, while the hydroxyl region is presented in Figure 4b. The FTIR spectrum of the as-synthesized sample shows intense bands at 1575, 1524, 1378 and 1280 cm^{-1}. These bands are identical to those reported in the literature for $[Cr(acac)_3]$ complexes grafted on silica[16] and can be attributed to the vibrations of the carbonyl and carbon–carbon double bonds in the conjugated chelate rings coordinated to the Cr^{3+} ion (Table 2). In the hydroxyl region, a broad band around 3400 cm^{-1} is observed, which is due to hydrogen bonding between surface hydroxyl groups and acac ligands. The FTIR spectra of the 1.00-Si-A sample do not change significantly up to a heating temperature of 200 °C. Above 200 °C, however, the acac bands and the broad band at 3400 cm^{-1} drastically decrease in intensity, and at 400 °C completely disappear. In contrast, the band at 3750 cm^{-1}, which corresponds to silanol groups, increases in intensity

0947-6539/00/0616-2962 $ 17.50+.50/0 *Chem. Eur. J.* **2000**, *6*, No. 16

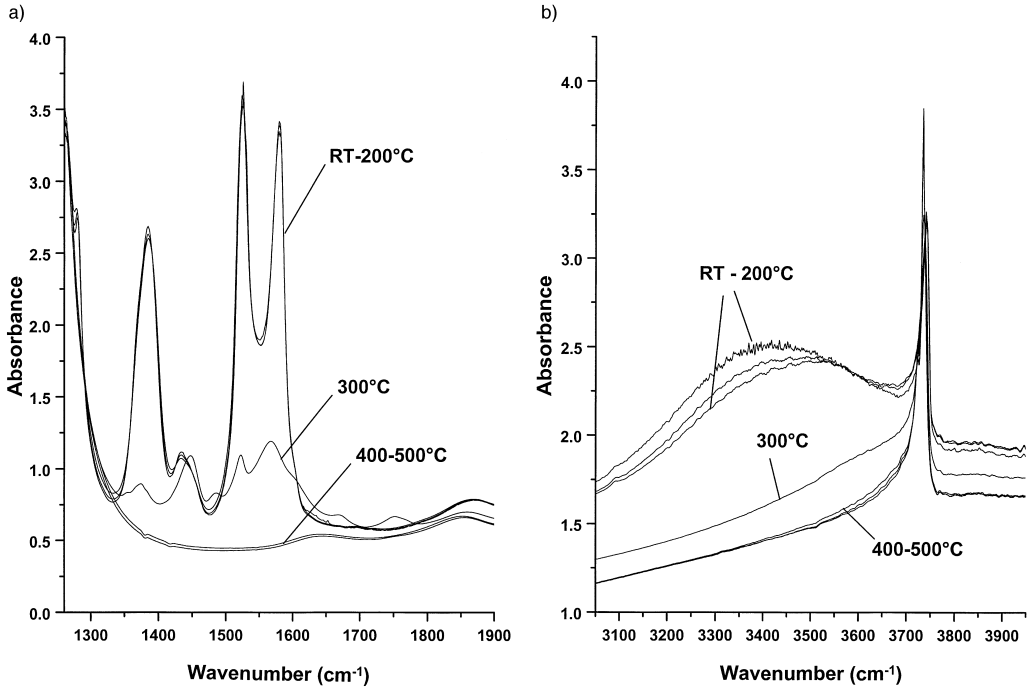

Figure 4. FTIR spectra of sample 1.00-Si-A: a) acac region and b) hydroxyl region, after heating in O_2 at 20, 200, 300, 400 and 500 °C.

Table 2. Assignments of the most important vibrations observed in the FTIR spectrum of 1.00-Al-A.

Wavenumber [cm^{-1}]	Assignment
1580	$\nu_s(CO)_{ring}$
1550	$2[\gamma(CH)]$
1530	$\nu_{as}(CCC)_{ring}$
1440	$\delta_{as}(CH_3)$
1400	$\nu_{as}(CO)_{ring}$
1370	$\delta_s(CH_3)$

with increasing calcination temperature. These FTIR results indicate that 1) almost no acac ligands are removed below 200 °C, 2) the major fraction of acac ligands is removed between 200 and 300 °C and 3) a small fraction of acac ligands remains on the surface at 300 °C. This is consistent with the TGA data of sample 1.00-Si-A (Figure 1a).

A series of FTIR spectra of the 1.00-Al-A sample obtained after different heat treatments in oxygen are shown in Figures 5a (acac region) and 5b (hydroxyl region). Similar

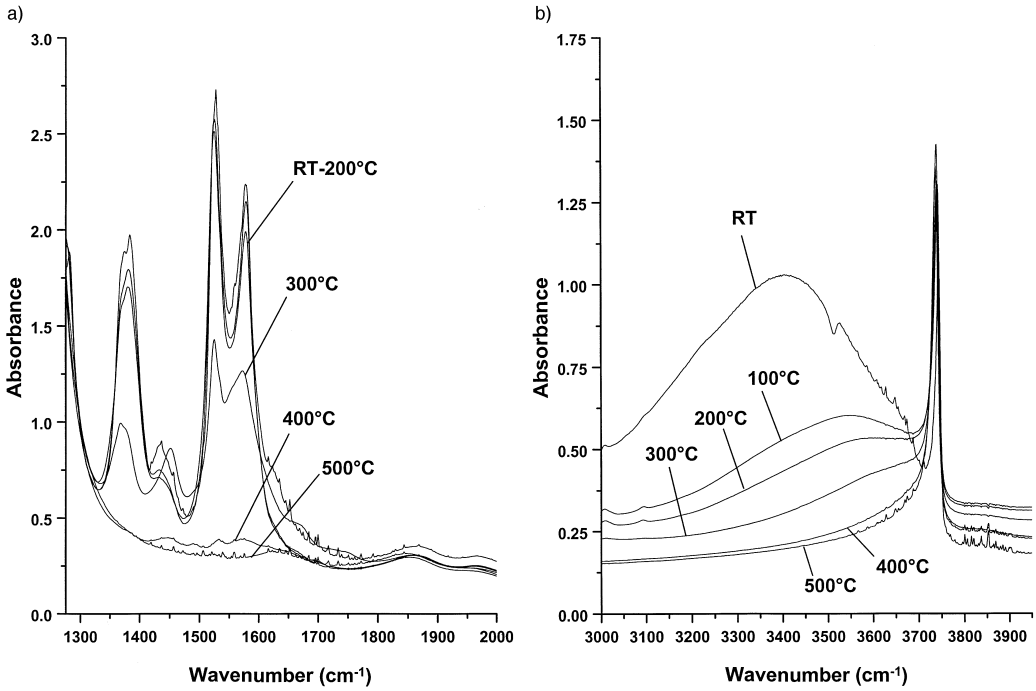

Figure 5. FTIR spectra of sample 1.00-Al-A: a) acac region and b) hydroxyl region after heating in O_2 at 20, 200, 300, 400 and 500 °C.

observations to those made for sample 1.00-Si-A can be made. However, the major difference between samples 1.00-Al-A and 1.00-Si-A is the relative decrease in intensities of the acac bands after heating the samples in oxygen. Indeed, the acac bands at 1575, 1524, 1378 and 1280 cm^{-1} are still clearly visible at 300 °C in the 1.00-Al-A material, whereas they are almost completely absent in the 1.00-Si-A sample. This means that for sample 1.00-Al-A 1) almost no acac ligands are removed below 200 °C, 2) about half of the acac ligands are removed between 200 and 300 °C and 3) the remaining fraction of acac ligands is removed between 300 and 400 °C. This is in full agreement with the TGA data of sample 1.00-Al-A (Figure 1a), and indicates a stronger interaction between [Cr(acac)$_3$] complexes and the Al-MCM-41 support.

In situ DRS spectra of sample 1.00-Si-A obtained after different heat treatments in oxygen are given in Figure 6. The spectrum of the as-synthesized sample obtained at room temperature is characterized by three absorption bands at 562, 389 and 327 nm, which are assigned to the three allowed d–d transitions of the deposited [Cr(acac)$_3$] complex with Cr^{3+} in a pseudo-octahedral coordination.[17, 18] This is schematically visualized in Figure 2. The spectra are recorded

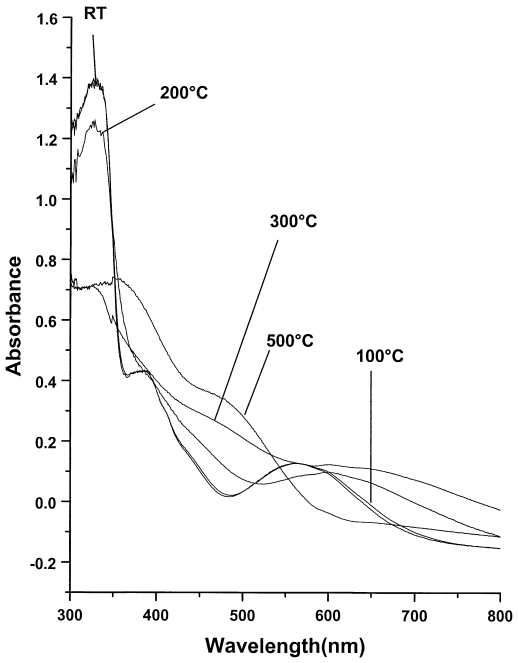

Figure 6. DRS spectra of sample 1.00-Si-A after heating in O_2 at 20, 200, 400 and 500 °C.

during calcination at temperatures of 100, 200, 300, 400 and 500 °C. The DRS spectrum measured at 100 °C is identical to that measured at room temperature. Increasing the temperature to 200 °C results in a shift of the first d–d band to 600 nm. This absorption band also shows shoulders at higher and lower energy; this indicates symmetry lowering of the Cr^{3+} site. Further heating to 300 and 400 °C in oxygen results in broad and ill-defined DRS spectra. At 500 °C the sample turns yellow-orange. The corresponding DRS spectrum has an absorption band at 360 nm and a shoulder at around 450 nm; these can be both assigned to the $O \rightarrow Cr^{6+}$ charge transfer transitions of dichromate and some chromate.[18, 19] These dichromate and chromate species are anchored onto the surface through an esterification reaction with the silanol groups of the MCM-41 material.

Analogeous DRS spectra were obtained for sample 1.00-Al-A (Figure 7). Thus, although a different anchoring mechanism is proposed for Cr-AlMCM-41 catalysts based on TGA and FTIR results, no significant differences in the absorption bands of the deposited [Cr(acac)$_3$] complex can be observed. The only difference with sample 1.00-Si-A is that the in situ DRS spectra of 1.00-Al-A measured at room temperature, 100 °C and 200 °C in oxygen are very similar, indicating that

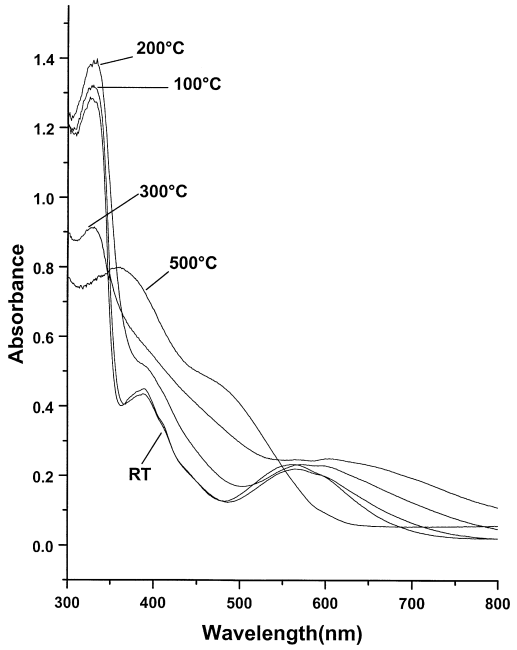

Figure 7. DRS spectra of sample 1.00-Al-A after heating in O_2 at 20, 200, 400 and 500 °C.

oxidation of the deposited [Cr(acac)$_3$] complexes to dichromate occurs at temperatures above 200 °C. This is indicative of a stronger interaction between [Cr(acac)$_3$] complex and the AlMCM-41 support. Similar observations were made for Cr-MCM-41 materials with higher Cr loadings, although these catalysts contain some Cr_2O_3 clusters after calcination, as evidenced by an absorption band around 600 nm.[18, 19] The latter observation implies that part of the Cr^{6+} cannot be stabilized on the surface through reaction with the silanol groups and is thermally converted into Cr_2O_3.

The ESR spectra of 1 wt % [Cr(acac)$_3$]-SiMCM-41 as a function of the calcination temperature are shown in Figure 8. The as-synthesized sample reveals an intense ESR signal with $g = 4.0$ and a weaker ESR signal at $g = 2$. These two ESR features correspond to a highly distorted Cr^{3+} species in octahedral coordination characterized by effective g values around 2.0 and zero-field parameters D and E equal to 0.45 and 0.15 cm^{-1}, respectively.[18, 20] Increasing the calcination temperature up to 200 °C results in a drastic decrease of the intensity of the ESR signal at $g = 4$ and the formation of a new

0947-6539/00/0616-2964 $ 17.50+.50/0 Chem. Eur. J. 2000, 6, No. 16

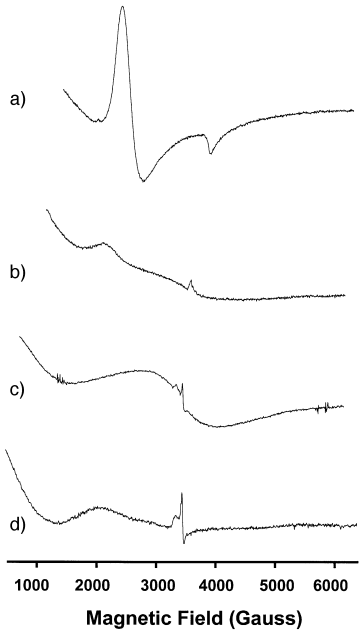

Figure 8. ESR spectra of sample 1.00-Si-A after heating in O_2 at a) 20 °C, b) 200 °C, c) 400 °C and d) 500 °C.

weak signal at around $g = 2$. This axially symmetric signal with $g_{\parallel} = 1.910$ and $g_{\perp} = 1.978$ is typical for square-pyramidal Cr^{5+}.[18, 20] In addition, a broad ESR signal centred at $g = 1.97$ is observed. This signal is typical for Cr_2O_3 clusters formed on the MCM-41 surface. This indicates that a fraction of the Cr^{3+} in deposited $[Cr(acac)_3]$ complexes cannot be stabilized at the MCM-41 surface after calcination and exists as dichromate and square-pyramidal Cr^{5+}. Similar observations were made for sample 1.00-Al-A, although the decomposition temperature of the deposited $[Cr(acac)_3]$ complex on AlMCM-41 starts well above 200 °C.

Ethylene polymerization with Cr-MCM-41 catalysts: Explorative catalytic experiments were performed in the gas phase at 100 °C and 2.2 bar initial ethylene pressure in a reactor. The Cr-MCM-41 catalysts were first pretreated at 550 or 720 °C for 2 h in oxygen and then transferred to the reactor. Table 3 summarizes the effect of the support composition, the initial calcination temperature and the Cr loading on the ethylene polymerization activity of Cr-MCM-41 materials. The following conclusions can be made: 1) the pure SiMCM-41 and AlMCM-41 materials have some activity in ethylene polymerization, 2) Cr-AlMCM-41 materials are more active then Cr-SiMCM-41 materials, 3) the catalytic activity increases with increasing Cr loading up to 1 wt% Cr for Cr-AlMCM-41 materials (higher Cr loadings result in less active materials) and 4) the catalytic activity increases with increasing initial calcination temperature. The latter observation is in line with those made for commercial Cr/SiO_2 catalysts.[21–24] Increasing calcination temperature usually gives rise to higher polymerization activity, which is explained by a change in the active-site bonding and coordination with the support surface. Another explanation can be the presence of support hydroxyl groups. The activity passes through a maximum with increasing dehydroxylation. An important factor influencing the degree of support dehydroxylation is the Cr loading. Since Cr and surface silanol groups react during catalyst activation by an anchoring mechanism, increasing Cr content increases dehydroxylation and thus catalyst activity.[18, 21, 25] The decrease in polymerization activity above 1 wt% Cr loading must then be due to the formation of Cr_2O_3 clusters on the MCM-41 surface, which are indeed observed with DRS and ESR. Another factor is the precalcination temperature. Higher temperatures effect a greater degree of hydroxyl removal, which favours catalyst activity.

Table 3. Gas-phase polymerization of ethylene over $[Cr(acac)_3]$-MCM-41 catalysts: effect of the support composition, calcination temperature and Cr loading.[a]

Catalyst	Activity[b] [g of PE per g of catalyst per h]
0.00-Al-C	7.80
0.50-Al-C	15.36
0.75-Al-C	25.62
1.00-Al-C	26.10
1.50-Al-C	7.44
2.00-Al-C	10.74
1.00-Al-C720	31.60
0.00-Si-C	6.00
1.00-Si-C	13.00

[a] Sample pretreatment = 550 °C or 720 °C for 2 h; amount of catalyst = 0.3 g; initial ethylene pressure = 2.2 bar; reaction temperature = 100 °C; reaction time = 2 h. [b] The activity is determined from the amount ethylene consumed during the whole ethylene polymerization run.

Further catalytic testing was done with the 1.00-Si-C and 1.00-Al-C catalysts in a reactor for slurry phase ethylene polymerization at 104 °C. The catalytic performances, together with the characteristics of the polyethylene formed, are given in Table 4. It is clear that the 1.00-Al-C sample is more than twice as active as the 1.00-Si-C catalyst and that the polymerization rate of the 1.00-Al-C catalyst is about 140 g polyethylene per gram of catalyst per hour, which is equivalent to 14000 g polyethylene per gram Cr per hour. This value has to be compared with an industrial Cr/SiO_2 catalyst, which under similar conditions produces about 1 kg of polyethylene per gram catalyst per hour.[21–24] Our catalytic performances are, however, much better than those previously observed for Cr-Y zeolites.[26–28] This must be due to the fact that the formation of polyethylene chains in the zeolite channels/pores is limited and that the chains block the active Cr sites after short polymerization runs. Because the zeolite materials do not readily break up during polymerization, low activities are usually observed. Indeed, it is known for Cr/SiO_2

Table 4. Slurry-phase polymerization of ethylene over $[Cr(acac)_3]$-MCM-41 catalysts.[a]

Catalyst	Activity[b] [g of PE per g of Cr per h]	Polymer characteristics MI5 [g per 10 min]	HLMI [g per 10 min]	SR5	bulk density [kg l^{-1}]
1.00-Al-C	14000	0.004	0.56	141	0.21
1.00-Si-C	6300	0.028	1.38	49	0.20

[a] Sample pretreatment = 650 °C for 6 h; amount of catalyst = 1.0 g; ethylene pressure = 31.4 bar; reactor temperature = 104 °C. [b] The activity is determined from the amount polyethylene formed during the whole ethylene polymerization run.

catalysts that if the silica structure is too rigid, fragmentation of the catalyst particle does not occur, the pores remain blocked by polymers, and no appreciable and long-standing polymerization activity is observed.[26–28] While the precise catalyst activity values are difficult to compare between the different catalysts reported in the open literature[21–28], we can conclude that our Cr-MCM-41 catalyst displays a substantial and long-standing polymerization activity.

The melt index of a potential polymerization catalyst is as important as its catalytic activity.[29] The melt index is a measure of the amount of molten polymer which can flow through a standard orifice under a set pressure in ten minutes. The plastics formed with our Cr-MCM-41 catalysts have high load melt flow indices (HLMI) of 0.56 and 1.38 g per ten minutes for the 1.00-Al-C catalyst and 1.00-Si-C catalyst, respectively. These low numbers, indicate a high molecular weight for the polyethylene formed (Table 4). The origin of this difference between catalysts is not yet clear. It may be caused by a different chemical composition (Si:Al ratio of ∞ vs. 27) or a different pore diameter of the MCM-41 material (28 Å vs. 25 Å) or a combination of both. Further studies will be directed towards a controlled change in the pore characteristics of the MCM-41 in order to investigate the effect of the pore diameter and pore volume on the polyethylene properties (melt index and molecular weight). In this respect, MCM-41s are very attractive supports for making novel polymerization catalysts because one can tailor the pore diameters of these materials by simply changing the length of the surfactant template molecule. The controlled introduction of Al and Ti in the MCM-41 structure will be a further scientific challenge.

XRD, DSC and FTIR have also been used to characterize the polyethylene formed by the 1.00-Al-C catalyst. The XRD pattern (Figure 9a) is typical of crystalline polyethylene with [110] and [200] diffraction peaks at 21.4° and 23.9°, respectively, while the weak shoulder at around 19.5° is due to amorphous polyethylene.[30] Thermal analysis of the polymer by DSC showed one single endotherm at 136 °C with the heat of fusion (ΔH) equal to 185 J g^{-1} (Figure 9b). Finally, FTIR indicated the characteristic vibrations at 721 (concerted rocking of CH_2 groups), 1463 (scissors band of CH_2 group) and 2926 cm^{-1} (antisymmetric stretching vibration of CH_2 group) of polyethylene.[31, 32]

Finally, it is important to stress that recently two studies by Howe et al. have appeared in the literature reporting on the polymerization of ethylene over Cr-MCM-41 materials.[33, 34] This group also observed that polyethylene was formed within the nanoscale one-dimensional channels of MCM-41 and that the polymerization activity was associated with the initial pressure of ethylene, the reaction temperature and the chromium loading.

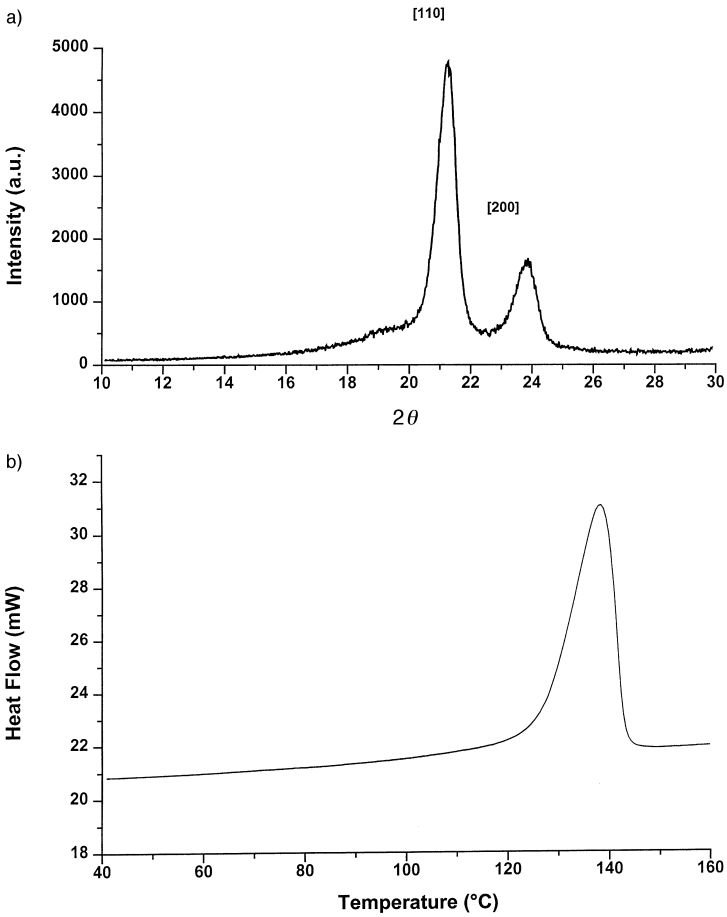

Figure 9. Characterization of polyethylene formed by sample 1.00-Al-C: a) XRD pattern and b) DSC melting curve.

Spectroscopy of a polymerizing Cr-MCM-41 catalyst: Ethylene polymerization was also carried out in a specially designed quartz flow cell equipped with an ESR tube and a DRS quartz window. A stream of pure ethylene gas at 100 °C was directed over a catalyst bed of 3 g of precalcined 1.00-Al-C material. Combined DRS-ESR spectroscopies were then used to monitor at regular time intervals the oxidation state and coordination environment of Cr in the polymerizing Cr-AlMCM-41 catalyst. As an example, we will discuss the obtained DRS spectra in some detail. A series of DRS spectra is given in Figure 10. The colour of the Cr-AlMCM-41 catalyst activated at 500 °C was yellow-orange and the corresponding DRS spectrum is characterized by absorption bands at 250, 342 and 450 nm, which can be assigned to dichromate.[18, 19] The broad shoulder in the range 550 – 800 nm is typical for the presence of small Cr_2O_3 clusters at the MCM-41 surface.[18, 19] The presence of such clusters is confirmed by the presence of an ESR signal centred at around $g = 1.97$ with a peak-to-peak width of more than 2000 G.[20] In addition, ESR indicates the presence of traces of Cr^{5+}. Introducing ethylene at 100 °C results in a gradual change in colour from yellow-orange to green-blue. The spectra show a gradual decrease of the intensities of the dichromate bands with increasing time-on-stream at the expense of a new band at 605 nm. Total reduction of Cr^{6+} to lower valent Cr species is only observed after two hours on stream, which indicates that there is an induction period for ethylene polymerization. The observation of such an induction period is in line with literature results on Cr/SiO_2 polymerization catalysts.[21, 25] The DRS band at 605 nm is indicative of the formation of Cr^{3+}, although the presence of Cr^{2+} species cannot be ruled out.[18] The presence of Cr^{3+} species in the active Cr-AlMCM-41 catalyst is confirmed by ESR spectroscopy. Indeed, the corresponding ESR spectrum is characterized by a broad ESR signal with

  0947-6539/00/0616-2966 $ 17.50+.50/0 *Chem. Eur. J.* **2000**, *6*, No. 16

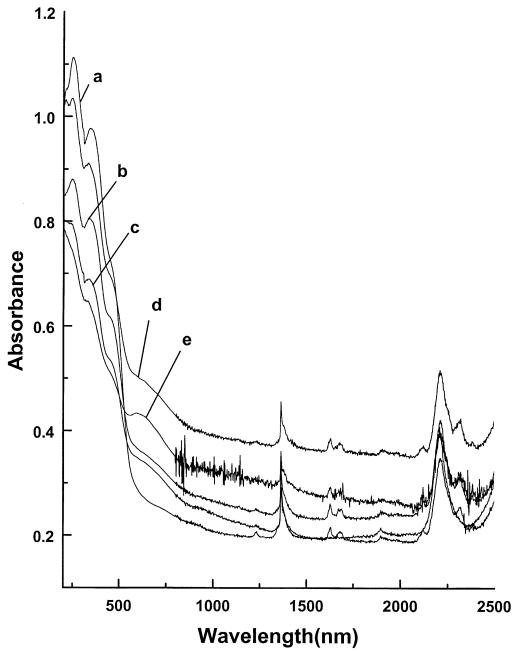

Figure 10. DRS spectra of sample 1.00-Al-A exposed to ethylene at 100 °C as a function of the reaction time: a) 0.17 h, b) 0.25 h, c) 0.5 h, d) 0.75 h and e) 2 h.

$g = 1.97$ and a peak-to-peak width of about 700 G. This Cr^{3+} ESR signal is different from that observed in the precalcined 1.00-Al-C sample, which indicates that a new (active) Cr^{3+} phase is formed during the induction period in the catalyst. In addition, a sharp signal at around $g = 2$ (due to Cr^{5+}) is still visible in the spectrum.

Another interesting feature of the DRS spectra of Figure 10 is the near infrared region, which shows overtone and combination bands of silanol groups and the polyethylene formed during catalysis. The absorption bands at 1237, 1363 and 2205 nm can be assigned to SiOH groups, while the absorption bands at 1632 nm (1st overtone of the antisymmetric stretch of CH_2 group), 1684 nm (1st overtone of symmetric stretch of CH_2 group), 2110 nm (4th overtone of the C–C stretch) and 2316 nm (combination of scissor and stretch bands of CH_2 group) are indicative of the formation of polyethylene.[31, 32] The formation of polyethylene in the quartz flow cell after two hours on stream was further confirmed by FTIR analysis of the final product. It reconfirmed that the polyethylene immediately fills the pores, resulting in fragmentation of the catalyst particles into smaller pieces, which continue to produce polymers. This gradual fragmentation gives rise to a continuous distribution of the Cr-MCM-41 material in the polyethylene formed.

Microscopy of a polymerizing Cr-MCM-41 catalyst: In another series of experiments, ethylene polymerization was carried out in a quartz flow cell at 100 °C and a stream of pure ethylene gas was directed over a catalyst bed of 1 g of precalcined 1.00-Al-C material. After 15 minutes of polymerization, the Cr-AlMCM-41 catalyst was poisoned with CO and ethylene polymerization immediately stopped. The Cr-AlMCM-41 material was removed from the cell and a catalyst granule (with dimensions of about $6 \times 4 \times 1.5$ mm) was selected and analysed with scanning electron microscopy (SEM) and electron microscope microprobe analysis (EMMA).

EMMA analysis of the catalyst granule at twelve different spots revealed the presence of Si, Al and traces of Cr. The Si:Al ratio was equal to 24, which is close to the value of the starting Cr-AlMCM-41 material[27]. However, EMMA is not sensitive for carbon, and thus this analysis technique could not reveal the presence of polyethylene.

SEM images of the catalyst granule are given in Figure 11. Figure 11a shows a lateral view of the catalyst granule. When the view was futher magnified (Figure 11b) small wormlike CrAlMCM-41 particles became visible, together with smaller particles of polyethylene. Further magnification shows a detailed view of the wormlike CrAlMCM-41 particles. Figure 11c reveals that the outer surface of the CrAlMCM-41 is rough and is (partially) covered by fibres of polyethylene. In the middle of Figure 11c, one can see a CrAlMCM-41 particle that is starting to break up. Bundles of polymer fibres of 50–100 nm thickness and and more than 1 μm length are clearly visible. Figure 11d shows the formation of nanofibres of polyethylene with a length of about 1 μm.

These results show that the polymer chains initially produced within the mesopores of the Cr-MCM-41 material form nanofibres of polyethylene with a length of several microns. Part of these nanofibres are protruding from the catalyst particle, while most of them (partially) cover the outer surface of the catalyst particles. These catalyst particles fragment further during ethylene polymerization.

Conclusion

The following conclusions can be drawn from this study:

1) The interaction of $[Cr(acac)_3]$ complexes with the surface of a SiMCM-41 support occurs through hydrogen bonding between surface hydroxyls and one or more acac ligands. The interaction of a $[Cr(acac)_3]$ complex with an AlMCM-41 support can, in addition, take place by a ligand exchange mechanism in which one of the acac ligands is replaced by framework oxygens or hydroxyl groups. The deposited $[Cr(acac)_3]$ complexes are more thermally stable on an AlMCM-41 support than on a SiMCM-41 support. Only small variations in d-spacing and pore characteristics are observed after grafting $[Cr(acac)_3]$ onto the MCM-41 surface and after calcination in oxygen at elevated temperatures.
2) As-synthesized $[Cr(acac)_3]$-MCM-41 materials contain Cr^{3+} ions in a strongly distorted octahedral coordination, which are gradually oxidized in oxygen to dichromate, some chromate and traces of square-pyramidal Cr^{5+}. These Cr species are stabilized onto the MCM-41 surface through an esterification reaction with the silanol groups of MCM-41. Some of the Cr cannot be stabilized on the surface as $Cr^{6+/5+}$ and is thermally converted to small clusters of Cr_2O_3.
3) Cr-MCM-41 materials are catalytically active in the gas- and slurry-phase polymerization of ethylene at 100 °C. The

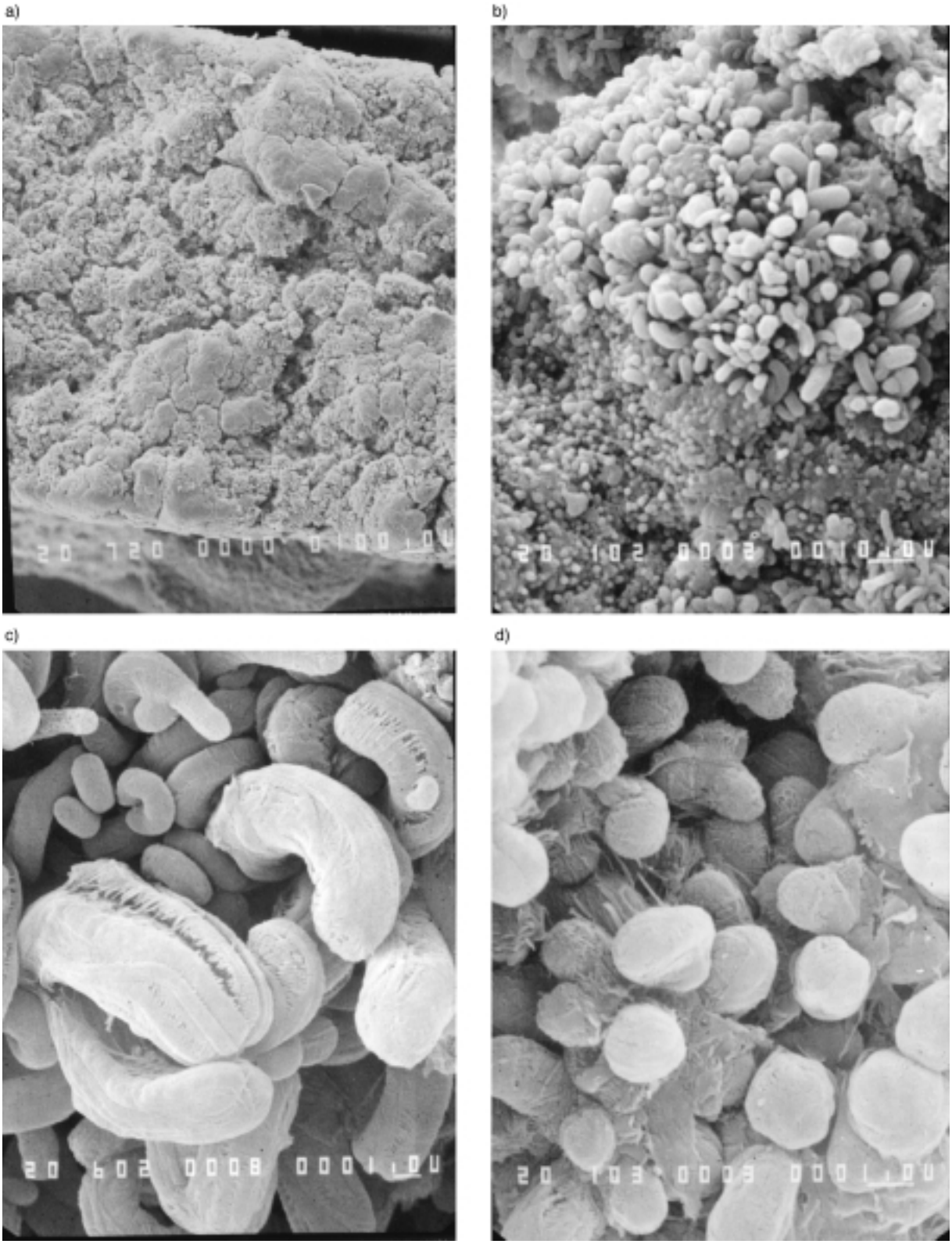

Figure 11. SEM images of a piece of an active 1.00-Al-C catalyst granule poisoned with CO at 100 °C: a) lateral view on a catalyst particle producing polyethylene, b) magnified view of (a), c) magnified view of b) showing Cr-MCM-41 particles and d) magnified view, showing Cr-MCM-41 particles.

catalyst activity is a function of the Cr loading, the calcination temperature and the support characteristics. 1 wt % $[Cr(acac)_3]$-AlMCM-41 treated at high temperature in oxygen is the most active catalyst with a polymerization rate of 140 g polyethylene per gram of catalyst per hour.

4) The Cr-MCM-41 catalyst shows an induction period, during which the catalytically inactive Cr^{6+} is mainly reduced to a Cr^{3+} species, characterized by a DRS absorption band at 605 nm and a broad ESR signal with $g = 1.97$ and a peak-to-peak width of about 700 G.

0947-6539/00/0616-2968 $ 17.50+.50/0 *Chem. Eur. J.* **2000**, *6*, No. 16

5) The polyethylene chains initially produced within the mesopores of the Cr-MCM-41 material form nanofibres of polyethylene with a length of several microns and diameter of 50 to 100 nanometers. These nanofibres (partially) cover the outer surface of the MCM-41 material. The catalyst particles gradually break up during ethylene polymerization, resulting in the formation of crystalline and amorphous polyethylene with a low bulk density and a high load melt flow index between 0.56 and 1.39 g per ten minutes.

Experimental Section

Catalyst preparation: The parent MCM-41 materials were prepared by using Ludox silica (AS-40) or TEOS (Acros) as the silicon source and $Al(OH)_3$ (Fluka) as the aluminium source, while TEAOH (tetraethyl ammoniumhydroxide, Aldrich) and HDTMABr (hexadecyltrimethyl ammoniumbromide, Merck) were used as template molecules. Pure silica MCM-41 (SiMCM-41) was prepared at room temperature according to a literature procedure.[35] Al-containing silica MCM-41 (AlMCM-41) was prepared by using the following modified literature procedure.[36] $Al(OH)_3$ (0.31 g), NaOH (0.3 g, Aldrich) and small amounts of bidistilled water were mixed together in a beaker and the solution was slowly heated. After obtaining a clear solution, TEAOH (9.26 g) was added to the cooled mixture. Ludox silica (9.26 g) was put in a separate beaker and stirred. Both solutions were mixed together at room temperature for 15 min, and HDTMABr (10.5 g) was added under continuous stirring. This final gel of composition $1\,Al_2O_3 \cdot 31\,SiO_2 \cdot 2.2\,(HDTMABr)_2O \cdot 3.16\,(TEA)_2O \cdot 1.89\,Na_2O \cdot 795\,H_2O$ was autoclaved at 100 °C for 24 h. The white, solid products were recovered by filtration, followed by washing (×3) with bidistilled water and drying at 60 °C in air. Finally, the materials were calcined in air at 550 °C for 24 h, cooled in N_2, and impregnated with a solution of a fixed amount of $[Cr(acac)_3]$ (Fluka) in methanol under N_2 atmosphere. The following Cr loadings were prepared: 0.0, 0.5, 0.75, 1.0, 1.5 and 2.0 wt %. An overview of the materials, their labelling and some of their properties is given in Table 1.

Physicochemical characterization: Electron microscope microprobe analysis (EMMA) was performed on a JEOL Superprobe 733 to determine the elemental composition of the catalysts. The Si:Al ratio of the AlMCM-41 material was 27. Powder XRD patterns of the as-synthesized and calcined materials were recorded with a Siemens D5000 X-ray diffractometer. DRS spectra were taken on a Varian Cary 5 diffuse reflectance spectrophotometer in the UV-Vis-NIR region at room temperature. A halon white reflectance standard was used as reference material. In situ DRS spectra were measured with the same spectrometer with a specially designed Praying Mantis diffuse reflectance attachment (Harrick). Details about this cell can be found in a recent paper.[37] The white reflectance standard $BaSO_4$ (Kodak) was used to take a baseline at 25 °C in the in situ cell. Thermogravimetric measurements (TGA) were performed in oxygen on a Mettler TG 50 thermobalance, equipped with a M3 microbalance and connected to a TC 10A processor. The heating rate was 10 °C min^{-1}. Porosity and surface-area studies were performed on a quantachrome autosorb-1-MP automated gas adsorption system. In situ FTIR measurements were done on a Nicolet 730 FTIR spectrophotometer with a specially designed in situ cell. The samples are measured as self-supporting wafers. EPR spectra were recorded at 300 and 120 K on a Bruker ESP 300E spectrometer operating in X-band (9.5 GHz). The polyethylene formed was characterized with FTIR, XRD, DSC, an extrusion plastometer or melt-flow indexer and SEM. SEM was performed with a Phillips 515 microscope. The melt-flow index (MI5, SR5 and HLMI) values were obtained from the resultant polyethylene at 190 °C according to ASTM procedures by using a SEAST extrusion plastometer.[38] The high load melt index (HLMI) index was determined with a weight load of 21.6 kg, while the melt index (MI5) was measured with a weight load of 5 kg. The SR5 index is defined as the ratio of HLMI and MI5.

Catalytic characterization: Explorative catalytic experiments were performed in the gas phase at 100 °C and at 2.2 bar initial ethylene pressure with 0.3 g of calcined catalyst in a 0.05 L stainless steel autoclave reactor, which was connected to a pressure gauge. The ethylene consumption and polyethylene formation were calculated from the pressure drop during ethylene polymerization. Further catalytic testing was done under slurry conditions with a bench-scale stainless steel 4 L stirred autoclave reactor. A pressurized jacket filled with boiling alcohol held the internal temperature of the reactor constant within 0.5 °C. About 1 g of catalyst was calcined in a quartz-tube activator at 650 °C for 6 h in dry air. After calcination, the catalyst was cooled to room temperature in dry nitrogen and the activated material was transferred to the empty reactor under a nitrogen flow. Then liquid isobutane (2 L) diluent was introduced in the reactor and the catalyst/isobutane suspension was continuously stirred (450 rpm). The reactor was heated to 104 °C and ethylene was introduced in the system. The reactor pressure (31.4 bar) was controlled in order to maintain 6 wt % ethylene dissolved in isobutane. Ethylene was added to the system through a mass-flow controller to maintain pressure during the reaction. The rate of ethylene polymerization was followed by monitoring the flow of ethylene into the reactor. The polymerization reaction was stopped after about 400 g of polyethylene was formed in the reactor.

Acknowledgements

R.R.R. is grateful for a junior postdoctoral fellowship of the K.U.Leuven, while B.M.W and P.V.D.V. are postdoctoral fellows of the Fonds voor Wetenschappelijk Onderzoek-Vlaanderen (F.W.O). O.C. acknowledges the Vlaams Instituut voor de Bevordering van het Wetenschappelijk – Technologisch Onderzoek in de Industrie (I.W.T.) for a PhD grant. The authors thank Hugo Leeman for performing the XRD, DSC and FTIR measurements of the polymers. This work was financially supported by the Geconcerteerde Onderzoeksactie (G.O.A.) of the Flemish Government and by the F.W.O. under grant No. G.0446.99.

[1] C. T. Kresge, M. E. Leonowicz, W. J. Roth, J. C. Vartuli and J. S. Beck, *Nature* **1992**, *359*, 710.
[2] J. S. Beck, J. C. Vartuli, W. J. Roth, M. E. Leonowicz, C. T. Kresge, K. D. Schmitt, C. T. W. Chu, D. H. Olson, E. W. Sheppard, S. B. McCullen, J. B. Higgins, J. L. Schlenker, *J. Am. Chem. Soc.* **1992**, *114*, 10834.
[3] J. Y. Ying, C. P. Mehnert, M. S. Wong, *Angew. Chem.* **1999**, *111*, 58; *Angew. Chem. Int. Ed.* **1999**, *38*, 56.
[4] D. Brunel, *Micropor. Mesop. Mater.* **1999**, *27*, 329.
[5] K. Moller, T. Bein, *Chem. Mater.* **1998**, *10*, 2950.
[6] A. Corma, *Chem. Rev.* **1997**, *97*, 2373.
[7] A. Corma, A. Martinez, V. Martinez-Soria, J. B. Monton, *J. Catal.* **1995**, *153*, 25.
[8] A. Tuel, *Micropor. Mesop. Mater.* **1999**, *27*, 151.
[9] N. Ulagappan, C. N. R. Rao, *Chem. Commun*. **1996**, 1047.
[10] W. Zhang, T. Pinnavaia, *Catal. Lett.* **1996**, *38*, 261.
[11] Z. D. Zhu, Z. X. Chang, L. Kevan, *J. Phys. Chem*. **1999**, *103*, 2680.
[12] M. Yonemitsu, Y. Tanaka, M. Iwamoto, *Chem. Mater.* **1997**, *9*, 2679; M. Yonemitsu, Y. Tanaka, M. Iwamoto, *J. Catal.* **1998**, *178*, 207.
[13] A. Poppl, P. Baglioni, L. Kevan, *J. Phys. Chem.* **1995**, *99*, 14156.
[14] R. Ramachandra Rao, B. M. Weckhuysen, R. A. Schoonheydt, *Chem. Commun*. **1999**, 445.
[15] S. Haukka, E. L. Lakomaa, T. Suntola, *Appl. Surf. Sci*. **1994**, *75*, 2220; A. Hakuli; A. Kytokivi, *Phys. Chem. Chem. Phys.* **1999**, *1*, 1607.
[16] I. V. Babich, Y. V. Plyuto, P. Van Der Voort, E. F. Vansant, *J. Colloid Interface Sci*. **1997**, *189*, 144.
[17] A. B. P. Lever, *Inorganic Electronic Spectroscopy*, 2nd ed., Elsevier, Amsterdam, **1984**.
[18] B. M. Weckhuysen, I. E. Wachs, R. A. Schoonheydt, *Chem. Rev.* **1996**, *96*, 3327.
[19] B. M. Weckhuysen, L. M. De Ridder, R. A. Schoonheydt, *J. Phys. Chem.* **1993**, *97*, 4756.
[20] B. M. Weckhuysen, R. A. Schoonheydt, F. A. Mabbs and D. Collison, *J. Chem. Soc. Faraday Trans.* **1996**, *92*, 2431.
[21] M. P. McDaniel, *Adv. Catal*. **1985**, *33*, 47.
[22] P. C. Thune, J. Loos, P. J. Lemstra, J. W. Niemantsverdriet, *J. Catal.* **1999**, *183*, 1.

[23] R. Merryfield, M. P. McDaniel, G. Parks, *J. Catal*. **1982**, *77*, 348.
[24] K. T. Choi, W. H. Ray, *J. Macromol. Sci. Rev. Macromol. Chem. Phys. C* **1985**, *25*, 1.
[25] B. M. Weckhuysen, R. A. Schoonheydt, *Catal. Today* **1999**, *51*, 215.
[26] J. K. Wang, T. Komatsu, S. Namba, T. Yashima, T. Uematsu, *J. Mol. Catal*. **1986**, *37*, 327.
[27] B. Wichterlova, Z. Traruzkova, L. Krajcikova, J. Novakova, *Structure and Reactivity of Modified Zeolites*, Elsevier, Amsterdam, **1984**, p. 246.
[28] Z. Tvaruzkova, B. Wichterlova, *J. Chem. Soc. Faraday Trans. 1* **1983**, *79*, 1591.
[29] M. P. McDaniel, D. R. Witt, E. A. Benham, *J. Catal.* **1998**, *176*, 344.
[30] S. Krimm, A. V. Tobolsky, *J. Polym. Sci.* **1951**, *7*, 57.
[31] C. N. R. Rao, *Chemical Applications of Infrared Spectroscopy*, Academic Press, New York, **1963**.
[32] C. N. Banwell, E. M. McCash, *Fundamentals of molecular spectroscopy*, 4th ed., McGraw-Hill, London, **1994**.
[33] J. He, F. Li, P. Sun, X. Duan, R. F. Howe, *Cuihua Xuebao*, **1998**, *19*, 588.
[34] J. He, X. Duan, R. F. Howe, *Huaxue Xuebao*, **1999**, *57*, 125.
[35] R. Mokaya, W. Jones, *Chem. Commun*. **1997**, 2185.
[36] J. Rathousky, A. Zukal, O. Franke, G. Schulz-Ekloff, *J. Chem. Soc. Faraday Trans*. **1994**, *90*, 2821.
[37] B. M. Weckhuysen, R. A. Schoonheydt, *Catal. Today* **1999**, *49*, 441.
[38] ASTM 1238–89: Standard test method for flow rates of thermoplastics by extrusion plastometer. Conditions for the melt index (MI5) and for the high load melt index (HLMI) are given in the procedures.

Received: November 15, 1999 [F2139]

  0947-6539/00/0616-2970 $ 17.50+.50/0